THE REACTION MECHANISM OF AMMONIA PRODUCTION VIA MAGNETIC INDUCTION METHOD: A DENSITY FUNCTIONAL THEORY (DFT) STUDY

Thien Duc Nguyen V., Mohamad Fakhrul Ridhwan Samsudin, Suriati Sufian*

Chemical Engineering Department,
Universiti Teknologi PETRONAS

Email: suriati@utp.edu.my

ABSTRACT

The iron (Fe) catalyzed hydrogenation of nitrogen molecule for the production of a green ammonia molecule was carried out via the B3LYP/6-31G (d,p) computational simulation in a room condition at 25°C. The results revealed that the first step of the nitrogen hydrogenation. At the same, the N atom is showing a lower barrier in comparison to different N atoms which results in a more favorable reaction. Furthermore, the most favorable isomerization observed was from trans to cis-Fe(HNNH) with an energy of 9.18 kcal/mol in relative to the trans-Fe(HNNH). In addition, the lowest activation energy was obtained from the system for the trans to cis isomerization. Moreover, the barrierless reaction was observed during the formation of the FeN2H4 molecule. Additionally, the rate determines the stage of the molecular reaction is the hydrogen addition to the nitrogen molecule at the same position with an activation energy of 36.80 kcal/mol.

Keyword: Haber-Bosch process, ammonia production, density functional theory, magnetic induction method, nanostructures.

INTRODUCTION

The ammonia production industry can be regarded as one of the most important chemical industrial due to its promising potential in a wide range of different applications such as sustainable fuel source, an efficient energy storage and as a green fertilizer [1], [2]. It is estimated that the total worldwide production of ammonia exceeded 140 million tons and the demand continues to grow due to the increasing demand from worldwide consumers [3]. In the past few decades, the Haber-Bosch process has been widely used in the production of ammonia [2]. However, this process requires a high temperature (300-500°C) and pressures (200-300 atm) for mitigating the sluggish kinetics reaction and ammonia decomposition phenomenon occurs during the reaction [4]. Moreover, the high energy input around 485 kJ mol^{-1} had caused a major setback in the Haber-Bosch process [3].

Recently, the magnetic induction method has been regarded as one of the most promising synthesizing methods in replacing the conventional Haber-Bosch process due to its low temperature and pressure requirement as well as high ammonia yield production [5]. With this new method, the Nano-catalyst and magnetic energy were employed to induce the catalytic activity while simultaneously optimized the production output. In lieu of the good features of this magnetic induction method, the optimum amount of magnetic strength that is required for diamagnetic H_2 addition reaction to N_2 still remain a boundless

challenge facing this magnetic approach [5]. Despite the many great works produced previously on the successful production of ammonia via this magnetic induction method, the study on the theoretical reaction mechanism, thermochemical parameters in the presence of the iron catalyst using the magnetic induction is relatively scarce. To the best of authors' knowledge, this is the first report specifically discussing the synthesis of ammonia via the magnetic induction method in the view of density functional theory study.

COMPUTATIONAL STUDY

There are many geometry optimizations of stationary points such as reactants, intermediates, complexed states, and products of N_2/H_2/Fe which runs using B3LYP/6-31G (d,p) at an open-shell system. All models are using the quintet multiplicity [6]. The frequency calculation is continuously similar to the theory of characterization of the thermochemistry parameters at minima points with the imaginary frequency of zero and maximum points with the imaginary frequency of 1. The scaled factor is used by 0.9806 with respect to the same theory. In order to eliminate the known systematic errors in the frequency calculation, an internal reaction coordination method is used to connect the minima points according to reaction paths. All the DFT calculations presented here are performed in the Gaussian 09 program [7].

RESULTS AND DISCUSSIONS

During the system simulation, the magnetic field is assumed to be stabilized at an open shell state of the system. The ground state of the system is denoted as a quintet state. It is expected to a minima magnetic strength that is required for the ammonia production. It is noteworthy to highlight that the exposure of Fe catalyst towards the molecular hydrogen will lead to a blockage of the active sites of catalyst, consequently limiting the catalytic reactions [7, 8]. The geometrical coordination position between Fe atom and the molecular nitrogen are located at an end and side-on bond. The DFT calculation results show that the ZPE of end-on coordination of 6.59 kcal/mol is larger than that of side-on coordination of 3.94 kcal/mol. This phenomenon leads to an increase in interatomic distance of N-N with 1.10 and 1.16 A^o, respectively. Moreover, the weakening bond of side-on coordination geometry is desirable as it is vital for the chemical activation of molecules [9]. On the other hand, the reaction between FeN_2 and $2H_2$ or $3H_2$ is unused due to the collisions of the three particles in the gas phase are hardly observed. In addition, the $(H_2)_2$ molecule are unable to survive at a room temperature (25°C) and the bonding energy observed is less than 0.1 kcal/mol [10].

Figure 1 depicts the potential energy diagram along with the different reaction pathway. Based on Figure 1, it can be deduced that there are two routes for the H_2 addition process to Fe/N_2, including the same N atom and different N atoms. For the similar N atom, an NNH_2 geometry structure is resulted from the hydrogenated dinitrogen via the transiting structure of TS1b. A TS1b relative to initial reactants lies 36.80 kcal/mol and the endergonic reaction is 21.99 kcal/mol.

Similarly, the endergonic reaction of 27.63 kcal/mol can be formed by the H_2 addition to different N atoms, leading to cis-Fe(HNNH) via the activated complex of TS1a with the energy of 58.04 kcal/mol linked to the $FeN_2 + H_2$ but not trans-Fe(HNNH) directly. However, the isomerization between trans and cis-Fe (HNNH) geometry occurs via the activation barrier of TS1c with an energy of 9.18 kcal/mol relative to trans-Fe (HNNH). Another isomerization occurs from Fe (NNH_2) to cis-Fe (HNNH) with transition state of TS1d, 52.09 kcal/mol and from Fe (NNH_2) to trans-Fe (HNNH) that has TS1e with energy barrier of 37.33 kcal/mol relative to $FeNNH_2$. Thus the most favorable isomerization is from trans to cis-Fe (HNNH).

In the activation energy comparison of H_2 addition to Fe/N_2, the hydrogenation of the same nitrogen is significantly more favorable than the different positions of nitrogen because the energy of TS1b is less than that of TS1a. The IRC calculations confirmed

that the transition state indeed verifies and connects with the reactants and products. Meanwhile, in the activated complex structure of TS1b, the N-H bonds are regularly formed with a distance of 1.02 A°, but a H-H bond (1.67 A) is actually broken. Initially, the Fe-N bond has a distance of 1.95 A°, however, the observed DFT analysis found that the present Fe-N bond in the system has a shorter distance in comparison to the original Fe-N bond. Consequently, resulting in the N-N bond elongation of 1.35 A°. In the structure of TS1a, the H-H is stretched to 2.52 A° and forming N-H bond is regularly 1.03 A while another NH bond is elongated to 1.53 A° where Fe-N is only formed via the short distance of 1.81 A°, leading to forming N=N quasi-double bond of 1.30 A°.

energy barrier that contains the transition state of $NNH_2 \rightarrow$ trans-N_2H_2 of 46.5 kcal/mol, cis$\rightarrow$trans-N_2H_2 of 44 or vice versa 48.8 kcal/mol [11]. Moreover, the polarization of the B3LYP/6-311G** shown that the activation energy of trans$\rightarrow$cis-N_2H_2 of 50.9 kcal/mol [12], B3LYP/6-311G (2d, 2p) of cis$\rightarrow$trans-N_2H_2 of 44.4 kcal/mol and $NNH_2\rightarrow$trans-N_2H_2 of 53.8 kcal/mol [13], respectively. Interestingly, the lowest activation energy of trans-to-cis isomerization performed in this study is lesser compared to the previous literature [11]-[13].

Another possible reaction is that the cis-Fe(HNNH) hydrogenation yielding Fe(H_2NNH_2) via TS2a with a barrier of 1.36 kcal/mol correlated to cis-Fe(HNNH) +

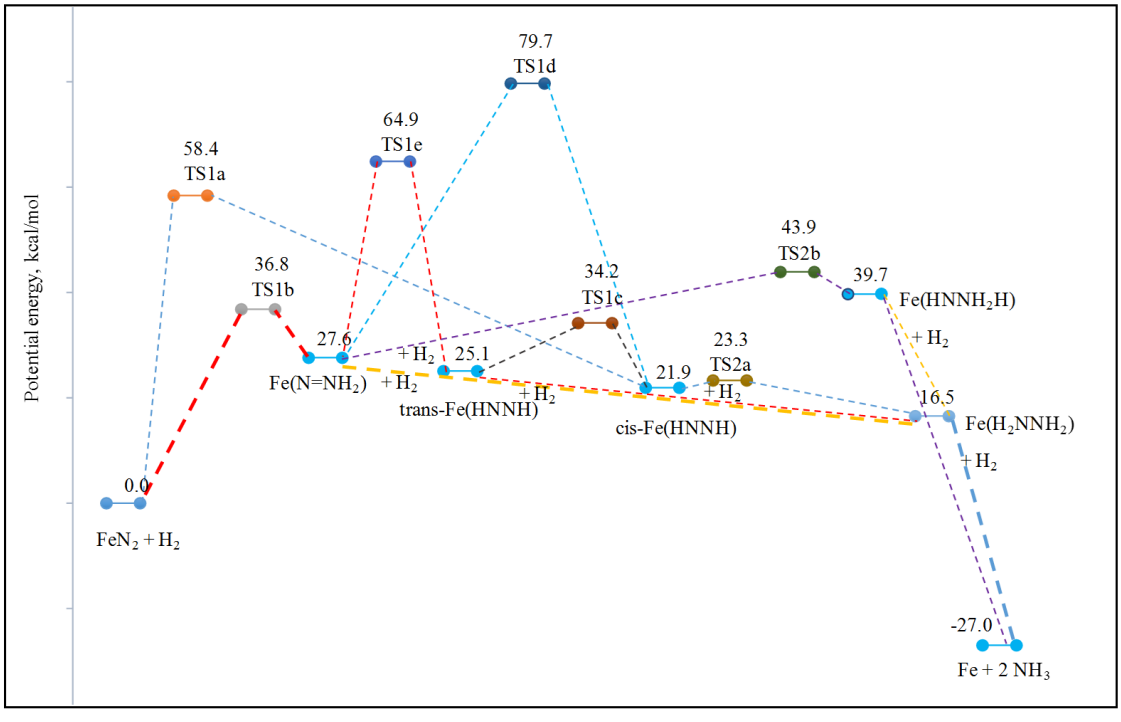

Figure 1 Full possible pathways for the Fe + N_2 + $3H_2 \rightarrow$ Fe +$2NH_3$ via B3LYP/6-31G(d.p) level of theory.

In the arrangement of cis and trans geometry, the formation of the N-H bond of 1.02 A° rotates around N-N bond of 1.46 A° that is larger than the N-N bond of cis-N_2H_2 geometry (1.34 A°). The formation of the Fe-N bonds of 1.84 A° in trans-geometry are shorter than 1.97 A° in cis-geometry that is unformed. Meanwhile, in the N_2H_2 system, without the presence of a catalyst, the study was performed using a singlet state. For example, G2M//MP2/6-31G** performs an

H_2 (as shown in Figure 2). For instance, the H-H bond in TS2a is stretched to 2.42 A° compared to isolated H_2 of 0.73 A°. The N-N bond is elongated by 0.1 A° and the Fe-N bond rupture increasing nearly twice in terms of the interatomic distance compared to those of cis-Fe(HNNH). All three types of various reaction pathways are the exergonic reaction of 3.25, 11.20, and 5.53 kcal/mol respectively. Additionally, another reaction pathway of Fe($HNNH_2H$) geometry is formed

by hydrogen addition to $Fe(NNH_2)$ via TS2b with a barrier of 16.59 kcal/mol. The endergonic reaction is calculated to be 14.63 kcal/mol. Adjusting the length of breaking H-H bond, 2.80 A° in TS2b, it is longer. However, the rupture distance of Fe-N bond is shorter than the TS2a. Furthermore, another isomerization of the FeN_2H_4 occurs between $Fe(HNNH_2H)$ and $Fe(H_2NNH_2)$ that is a spontaneous reaction because the activated energy that carries a negative value of 0.23 kcal/mol.

The last step of the hydrogen addition to FeN_2H_4 occurs via a two reaction pathways. Based on the DFT analysis, there are two types of N_2H_4 geometry including the H_2NNH_2 and $HNNH_2H$. However, in order to produce the NH_3, both pathways of reaction cause an exergonic reaction with respect to their reaction energy of 48.82 and 66.72 kcal/mol. These processes take place via an activated complex which performs a negative energy of activation barrier of 30.77 and 37.94 kcal/mol relative to Fe (H_2NNH_2) and

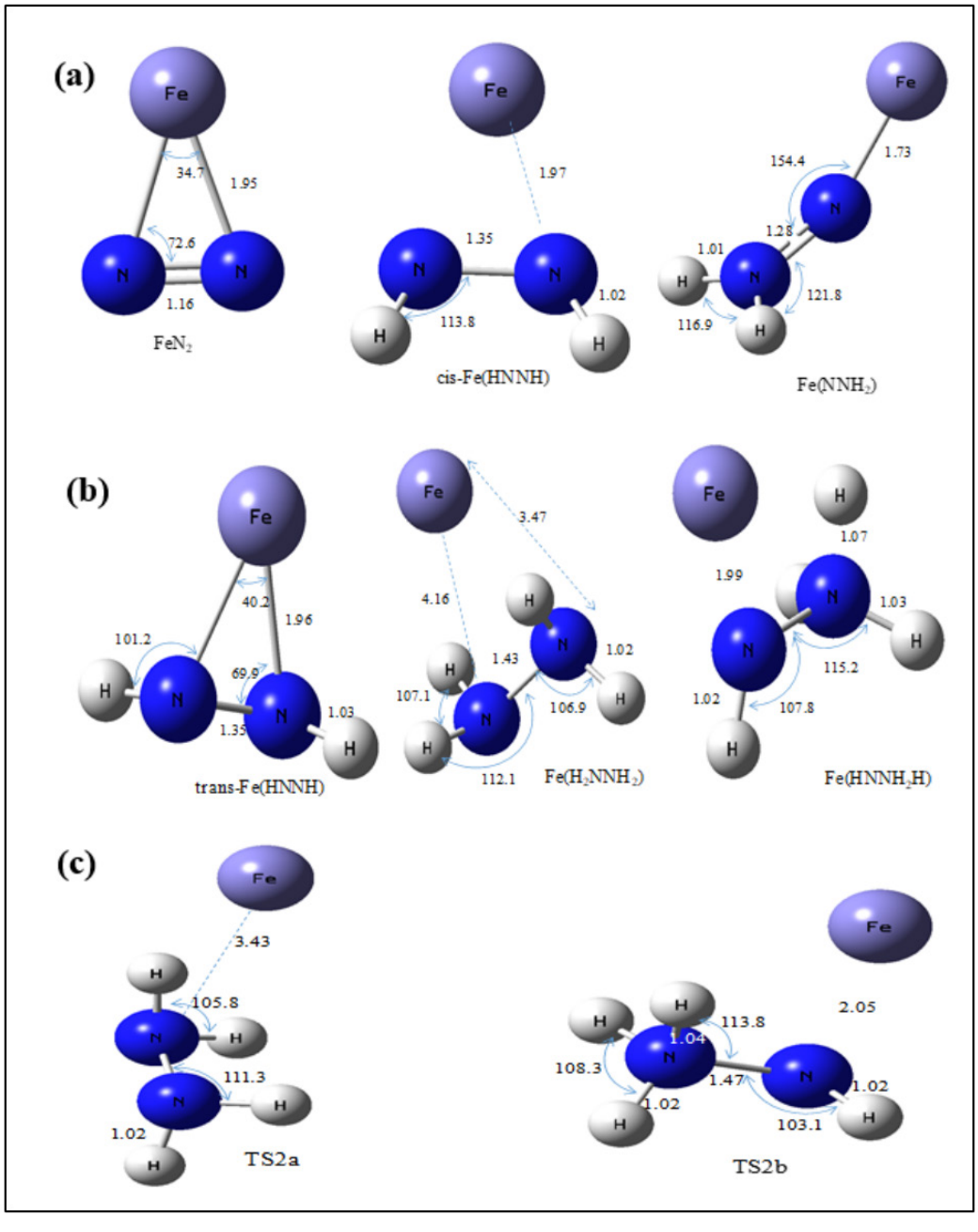

Figure 2 List of geometries of intermediates, transition states, reactants and products of the Fe + N_2 + $3H_2$ ⟶ Fe +$2NH_3$ via B3LYP/6-31G(d.p) level of theory

Fe($HNNH_2H$) respectively. This means that the H_2 addition to $HNNH_2H$ and H_2NNH_2 plays an important role of typically barrierless reactions in the last step. Both exergonic reactions represent a rupture of N-N bond via an activated complex structure.

The N-N bond is elongated to 3.65 A° in the nitrogen hydrogenation of $HNNH_3$ and it is larger than the N-N bond of 3.09 A° based on hydrogen addition to H_2NNH_2. The regular formation of the N-H bond is 1.02 A° but the H-H bond, which is stretched to

Table 1 The relative energies of various elements in N_2/H_2/Fe system over B3LYP/6-31G (d,p)

Species	relative energy	Relative reaction energy	relative energy barrier
$FeN_2 + H_2$	0		
TS1a	58		58
TS1b	36.8		36.8
cis-Fe(NHNH)	21.9	21.9	
TS1d	79.7		52.1
Fe(N=NH_2)	27.6	27.6	
TS1c	34.2		9.2
TS1e	64.9		37.3
trans-Fe(HNNH)	25.1	25.1	
TS2a	23.3		1.3
TS2b	23.8		-3.8
TS2c	23		-2.1
TS2d	43.9		16.3
Fe(H_2NNH_2)	16.5	-5.5 (relative to cis-Fe(NHNH))	
		-11.2 (relative to Fe(NNH_2)	
		-3.2 (relative to trans-Fe(HNNH)	
TS2e	39.4		-0.23
Fe(H_2NNH2)	39.7	12 (relative to Fe(NNH_2))	
		17.7 (relative to cis-Fe(NHNH))	
TS3a	-14.3		-30.8
TS3b	-21.6		-37.9
Fe + $2NH_3$	-27	-48.8 (relative to Fe(H_2NNH_2))	
		-66.7 (relative to Fe($HNNH_2H$))	

1.62 and 3.88 A° consequently, is broken during this reaction. However, both Fe-N bonds are not formed and an interatomic distance of 2.18 and 3.48 A° in hydrogenation to $HNNH_2H$ has a shorter than those of the 3.50 and 3.51 A° in hydrogen addition to H_2NNH_2. These results from the FeN_2H_4 formation and $Fe + 2NH_3$ final step are opposite to Hwang's result with larger energy barrier above 30 kcal/mol, using BeO catalyst or no catalyst [11], [14]. In this research, the total reaction energy of ammonia production is an exergonic reaction of 27.03 kcal/mol relative to the initial reactants of $FeN_2 + 3H_2$. Table 1 summarized the relative energies of various elements in $N_2/H_2/Fe$ system calculated at the B3LYP/6-31G(d,p) levels of theory.

CONCLUSION

The molecular reaction mechanism with Fe catalyzed hydrogenation of nitrogen molecule producing ammonia molecule is carried out using the B3LYP/6-31G(d,p) computational simulation in a room condition at 25°C. The results display that first step of hydrogen addition to the same N atom is lower compared to those of different N atoms. However, in the next stage of the FeN_2H_4 formation, the barrierless reaction occurs but other transition states with a low barrier is present at TS2a and TS2b. Finally, the last step is to be barrierless in order to produce ammonia. The most favourable reaction pathways in the molecular reaction contains $FeN_2 + H_2 \rightarrow$ TS1b $\rightarrow FeNNH_2$ with Ea=36.80 kcal/mol, $FeNNH_2 + H_2 \rightarrow FeH_2NNH_2$, $FeH_2NNH_2 + H_2 \rightarrow Fe + NH_3 + NH_3$. The rate-determining stage of the molecular reaction is the addition of hydrogen to the nitrogen molecule at the same position. Therefore, to produce ammonia as simulation, the minimum external energy required should be equal to the activated energy during the first step of the nitrogen hydrogenation.

ACKNOWLEDGEMENT

The authors would like to express their appreciation to the Chemical Engineering Department, Universiti Teknologi PETRONAS and Ministry of Higher Education Malaysia for the financial and laboratory support under FRGS (0153AB-I99).

REFERENCES

[1] Y. Bicer & I. Dincer, "Life cycle assessment of nuclear-based hydrogen and ammonia production options: A comparative evaluation", *International Journal of Hydrogen Energy,* vol. 42, pp. 21559-570, 2017.

[2] C. Chen, H. Aryafar, K.M. Lovegrove, & A.S. Lavine. "Modelling of ammonia synthesis to produce supercritical steam for solar thermochemical energy storage", *Solar Energy,* vol. 155, pp. 363-371, 2017.

[3] M.A. Shipman & M.D. Symes, "Recent progress towards the electrosynthesis of ammonia from sustainable resources", *Catalysis Today,* vol. 286, pp. 57-68, 2017.

[4] P. Peng, P. Chen, C. Schiappacasse, N. Zhou, E. Anderson, D. Chen, J. Liu, Y. Cheng, R. Hatzenbeller, M. Addy, Y. Zang, Y. Liu & R. Ruan, "A review on the non-thermal plasma-assisted ammonia synthesis technologies", *Journal of Cleaner Production,* vol. 177, pp. 597-609, 2018.

[5] B. Alqasem, N. Yahya, S. Qureshi, M. Irfan, Z.U. Rehman, & H. Soleimani, "The enhancement of the magnetic properties of α-Fe_2O_3 nanocatalyst using an external magnetic field for the production of green ammonia", *Materials Science and Engineering B,* vol. 217, pp. 49-62, 2017.

[6] A. T. Baryshnikova, B. F. Minaev, G. V. Baryshnikov & H. Agren, "Computational study of the structure and magnetic properties of the weakly-coupled tetranuclear square-planar complex of Cu(II) with a tetraporphyrin sheet" *Inorganica Chimica Acta,* vol 485, pp 73-79, 2019. doi.org/10.1016/j.ica.2018.09.086.

[7] J. Wang, S. Zeng, F. Huo, D. Shang, H. He, L. Bai, X. Zhang & J. Li, "Metal chloride anion-based ionic liquids for efficient separation of NH_3", *Journal of Cleaner Production,* vol. 206, pp. 661-669, 2019.

[8] P. Moggi, G. Albanesi, G. Predieri & G. Spoto, "Ruthenium cluster-derived catalysts for ammonia synthesis", *Applied Catalysis A: General.* vol. 123, pp. 145-159, 1995.

[9] I.B. Bersuker, *Electronic structure and properties of transition metal compounds: introduction to the theory,* John Wiley & Sons, 2010.

[10] V.M. Rozenbaum, A. Mebel, & S. Lin, "Intermolecular potential and equilibrium orientational states for dimers of non-polar molecules", *Molecular Physics,* vol. 99, pp. 1883-1897, 2001.

[11] D. Y. Hwang & A. M. Mebel, "Reaction Mechanism of N_2/H_2 conversion to NH_3: A theoretical study", *Journal of Physical Chemistry A,* vol. 107, pp. 2865-2874, 2003.

[12] P.K. Chattaraj, P. Perez, J. Zevallos & A. Toro-Labbe, "Theoretical study of the trans-N_2H_2 → cis-N_2H_2 and F_2S_2 → FSSF reactions in gas and solution phases", *Journal of Molecular Structure: Theochem,* vol. 580, pp. 171-182, 2002.

[13] B.S. Jursic, "Ab initio and density functional theory study of the diazene isomerization", *Chemical Physics Letters,* vol. 261, pp. 13-17, 1996.

[14] D.Y. Hwang & A.M. Mebel, "Reaction mechanism of the synthesis of ammonia in the N_2/H_2/FeO systems: A theoretical study", Journal of Physical Chemistry A, vol. 107, pp. 5092-5100, 2003.

AUTHORS' INFORMATION

Thien Duc Nguyen V received his PhD from Universiti Teknologi PETRONAS, Malaysia in 2017 under supervision of Associate Professor Dr. Suriati Sufian. His major research interest is in the development of advanced materials, particularly in carbon nanofibers for ammonia production.

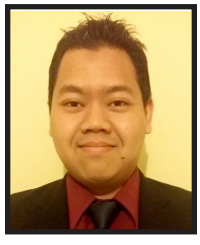

Mohamad Fakhrul Ridhwan Samsudin received his Bachelor and Master degree in chemical engineering from the University of New South Wales, Australia (2016) and Universiti Teknologi PETRONAS, Malaysia (2018), respectively. Currently, he is a PhD student under the supervision of Associate Professor Dr. Suriati Sufian. His major research interest includes the development of advanced materials such as graphene and carbon nanotubes, and photocatalyst materials for a wide range of photocatalytic applications.

Suriati Sufian is an Associate Professor affiliated with Department of Chemical Engineering at Universiti Teknologi PETRONAS, Malaysia. Her research area focuses on advanced renewable energy through the approach of materials and engineering design. She interested in development of carbon nanotube (CNT) and graphitic nanofiber (GNF) (also known as carbon nanofiber or CNF) for hydrogen storage applications. Then, she extended her CNT and CNF applications in others like catalyst support (for hydrogen production), wastewater treatment (dye removal and heavy metal removal), etc. and also nano metal oxides application in photocatalysts.